

On-Chip Functionalization of Carbon Nanotubes with Photosystem I

Simone M. Kaniber,[†] Matthias Brandstetter,[†] Friedrich C. Simmel,[‡] Itai Carmeli,^{*,§} and Alexander W. Holleitner^{*,†,‡}

Walter Schottky Institut, Technische Universität München, Am Coulombwall 3, D-85748 Garching, Germany,
Physik-Department, Technische Universität München, James Franck Strasse 1, D-85748 Garching, Germany, and
Department of Chemistry, Tel-Aviv University, 69978 Tel-Aviv, Israel

Received December 22, 2009; E-mail: itai@post.tau.ac.il; holleitner@wsi.tum.de

Photosynthesis in plants and bacteria is driven by molecular electronic complexes, such as the photosystem I (PSI).¹ Photoexcitation of PSI causes an electron transfer through a series of redox reactions from the chlorophyll special pair P700, as a primary electron donor, to a final electron acceptor, ~ 6 nm away from the oxidant P700.^{1–3} The resulting photopotential is ~ 1 V, and the intrinsic conversion of solar energy to electrical energy has an efficiency of $\sim 58\%$.^{1,2,4} These properties make the PSI a promising building block in nanoscale optoelectronic devices.^{5,6} Recently, the electronic and optoelectronic properties of PSI have been investigated in oriented self-assembled monolayers on top of gold^{2,3} as well as GaAs⁷ surfaces. Here, we study the optoelectronic properties of carbon nanotube (CNT)-PSI hybrids for three different on-chip functionalization strategies. The PSI is bound to the CNTs via covalent, hydrogen, or electrostatic bonds. The covalent bonding is achieved via selectively generated cysteins on the luminal side of the PSI. We find that optoelectronically active junctions between PSI and the CNTs are only achieved in cases where the electron transfer path of the PSI is perpendicular to the CNTs.

For all three approaches, we use single-walled CNTs (from Arry, Nanomaterials and Nanotechnology) with a diameter in the range 1–2 nm and either semiconducting or metallic properties.^{8,9} As in various hybrid nanosystems,^{10–13} the CNTs serve as nanoscale electrical wires in the presented PSI-CNT hybrids. For device fabrication, individual carboxylated CNTs are first deposited on an insulating SiO₂ substrate and then contacted with Pd source–drain electrodes by e-beam lithography.¹⁰ For the first chemical route, amine reactive NHS-esters are generated at the carboxyl groups of the CNTs which are reacted with ethylenediamine (Pierce) and a second linker molecule sulfo-MBS (Pierce). After activation of the thiol cysteins on the luminal side of the genetically mutated PSI² with dithiothreitol (Sigma-Aldrich), the chip with maleimide functionalized CNTs is immersed overnight in the protein solution. Afterward, the sample is rinsed with deionized water and dried under nitrogen.

AFM images (Figure 1a–c) before and after functionalization of the CNTs with PSI provide a first indication that PSI proteins are attached to the sidewalls of the CNTs. The diameter of the CNTs is ~ 2 nm, according to the height profile in Figure 1d. After chemical treatment a large number of spherical particles is attached to the same CNT (Figure 1b and 1c). One particle on the sidewall of the CNT is highlighted by a circle in Figure 1c, which displays a magnification of the dashed square in Figure 1b. The diameter of the particles is in the range 15–22 nm (see height profile in Figure 1e), which is consistent with the diameter of the PSI.¹ We interpret the findings as PSI proteins attached to the sidewall of the CNT due to covalent bonding between the maleimide functionalized CNT

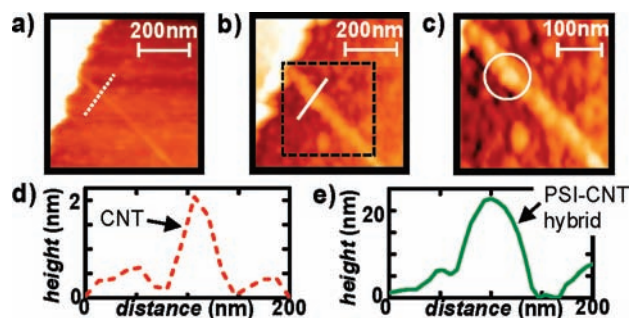


Figure 1. Atomic force microscope (AFM) image of a contacted CNT (a) before and (b) after chemical treatment for covalently binding the PSI to the CNT. (c) Enlarged image of dashed square in Figure 1b, showing a large number of PSI bound to the sidewall of the CNT. (d) and (e) Single traces along the dotted and solid lines in Figure 1a and 1b.

and selectively generated cysteins on the luminal side of the PSI.^{2,14,15} Hence, the electron transfer path in PSI is perpendicular to the CNT (sketch in Figure 2a).

For optoelectronic measurements, a bias voltage V_{SD} is applied across the source–drain electrodes and the light of a titanium:sapphire laser is focused through an objective of a microscope onto the CNT based circuits. All measurements are performed at $p < 1 \times 10^{-3}$ mbar.^{10,14,15} The electrical signal is amplified by a current–voltage converter (Ithaco 1211) and read out with a lock-in amplifier (eg&g 7260). The latter detects the current difference for the laser being “on” and “off”, $\Delta I = I_{ON} - I_{OFF}$, at the trigger frequency of the optical chopper, f_{CHOP} , in the kHz regime. Due to the fact that the examined circuits show an ohmic behavior for small V_{SD} (up to 100 mV) their photoconductance can be estimated by $G_{PH} = \Delta I/V_{SD}$. Filled squares in Figure 2a depict the wavelength dependence of the photoconductance of sample A, which was fabricated by the first chemical route. The photoconductance shows an enhanced signal at 680 and 360 nm. The findings are consistent with the absorbance data of the PSI (solid line in Figure 2a) which were taken in solution (Jasco V-550 UV–vis spectrophotometer). The origin of the enhanced photoconductance at the resonances of the PSI can be attributed to an electron or energy transfer between the excited PSI and the CNTs. A charge (energy) transfer exhibits slow (fast) photoconductance dynamics.¹⁵ Both dynamics can be detected in the presented single PSI-CNT hybrid system. With respect to the absorption of unbound PSI in solution, the expected photoconductance at ~ 420 nm is either slightly suppressed or blue-shifted. This can be caused by the interaction between PSI and the solid state surface, as first reported for PSI immobilized on Au surfaces.⁴

Importantly, the enhanced G_{PH} below 700 nm can be attributed to an effect of the PSI. This is proven by measurements on sample B (Figure 2b). Here, the photoconductance of a CNT bundle before (○) and after (■) on-chip functionalization with PSI by covalent

[†] Walter Schottky Institut, Technische Universität München.

[‡] Physik-Department, Technische Universität München.

[§] Department of Chemistry, Tel-Aviv University.

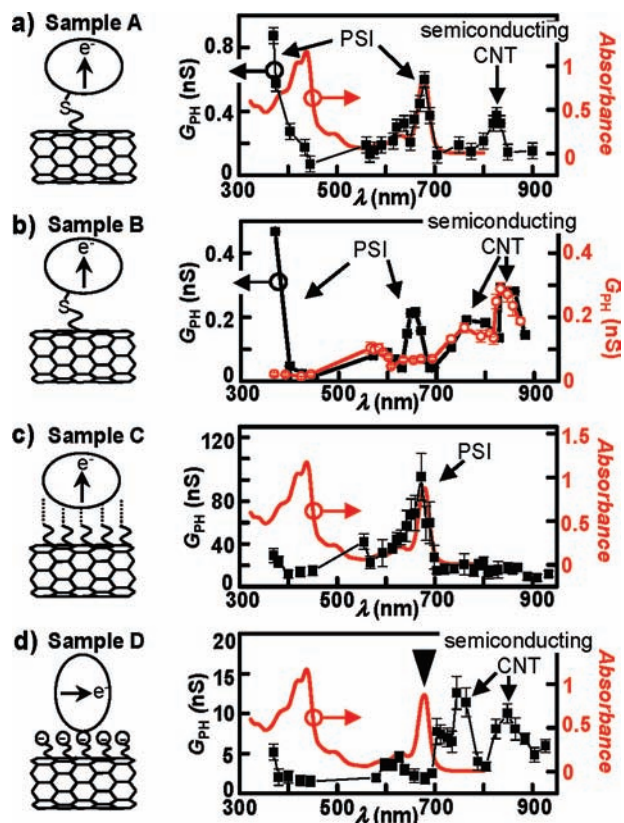


Figure 2. (a) Wavelength dependence of the photoconductance of sample A (\blacksquare , $P_{\text{LASER}} = 127 \text{ W/cm}^2$), where the PSI is covalently bound to the CNT with its electron transfer path perpendicular to the CNT. (b) Equivalent data for sample B, before (\circ) and after (\blacksquare) on-chip functionalization by covalent linkage ($P_{\text{LASER}} = 81 \text{ W/cm}^2$). (c) Data for sample C (\blacksquare , $P_{\text{LASER}} = 2.9 \text{ kW/cm}^2$) where PSI is attached to amine modified CNTs. (d) Data for sample D (\blacksquare , $P_{\text{LASER}} = 955 \text{ W/cm}^2$), where the electron transfer path is expected to be oriented parallel to the CNTs due to Coulomb interactions. The absorbance of the PSI is plotted as a solid line in Figure 1a, c, and d.

bonding is compared. The maxima at 680 nm and at ~ 360 nm only appear when the PSI is attached to the CNTs. Above 700 nm, the PSI does not absorb light, and in turn, the magnitude of the photoconductance before and after functionalization with PSI is the same within the experimental error. Consequently, the two photoconductance maxima around 760 and 845 nm and also the maximum at 825 nm in Figure 2a are interpreted to result from electron-hole dynamics only within the contacted CNTs.^{15–18} These findings are consistent with resonances assigned to the E_{22} transition in semiconducting CNTs with a diameter in the range 1–2 nm.^{10,15,17}

In the second chemical route, the electrically contacted CNT bundle of sample C is functionalized with ethylenediamine. After activation of the cysteins at the PSI with dithiothreitol, sample C is incubated in a PSI solution at pH 7.2. In analogy to Figure 1b, AFM measurements prove that the PSI is adsorbed to the CNTs (data not shown). This can be explained by hydrogen bond formation or electrostatic interactions between the PSI and the amino groups on the CNTs which are positively charged at pH 7.2. In both cases, the PSI is preferentially orientated with its electron transfer path perpendicular to the amine modified CNTs³ (sketch in Figure 2c). The photoconductance of sample C shows a peak at 680 nm (Figure 2c) which again can be assigned to a charge or energy transfer between the PSI and the CNT.¹⁵ The increase in photoconductance at ~ 360 nm, however, is only weak. Above 700

nm, no photoconductance resonances are observed, which is consistent with the fact that the I - V characteristic of this hybrid shows a metallic behavior (data not shown), and in turn, the CNT is metallic.⁸

In the third chemical route (sample D), the functionalization of the CNTs with PSI is enabled by electrostatic forces between negatively charged terminal groups on the CNTs and positively charged regions on the luminal and stromal side of the PSI.³ By incubating the chip with the contacted, carboxylated CNTs in a buffer solution at pH 7.2, the carboxyl groups are deprotonated resulting in negatively charged COO^- groups.³ Then, PSI is added. After ~ 12 h, the sample is rinsed with deionized water and dried under nitrogen. AFM measurements demonstrate a partial adsorption of PSI to the CNTs (data not shown). The wavelength dependent photoconductance of sample D (squares in Figure 2d), however, shows only resonances above 700 nm which are caused by electron-hole dynamics in semiconducting CNTs.^{15–18} The slightly enhanced photoconductance around 600 nm can be assigned to CNTs (compare Figure 2b). Most importantly, there is no photoconductance resonance at 680 nm (triangle in Figure 2d), a fact which can be explained by a less efficient adsorption of the PSI to the CNTs and by considering the mechanism of adsorption of the PSI on the CNTs. Electrostatic interactions between negatively charged COO^- groups and the PSI favor a parallel orientation of the PSI's electron transfer path with respect to the CNT.³ For this alignment the photogenerated dipole is parallel to the CNTs' axis and the proposed mechanism of energy transfer¹⁵ is less efficient.¹⁹ In addition, a possible charge transfer between the PSI and the CNT¹⁵ is suppressed in this configuration.

We have studied the functionalization of 17 carbon nanotube devices plus 22 nonfunctionalized devices for control measurements. We find that a perpendicular orientation of the electron transfer path within the PSI with respect to the CNT is crucial for an efficient optoelectronic functionalization of CNTs.

Acknowledgment. We acknowledge support by the DFG via Grant HO3324 and the Nanosystems Initiative Munich (NIM).

References

- (1) Brettel, K. *Biochim. Biophys. Acta* **1997**, *1318*, 322.
- (2) Frolov, L.; Rosenwaks, Y.; Carmeli, C.; Carmeli, I. *Adv. Mater.* **2005**, *17*, 2434.
- (3) Lee, I.; Lee, J. W.; Greenbaum, E. *Phys. Rev. Lett.* **1997**, *79*, 3294.
- (4) Carmeli, I.; Frolov, L.; Carmeli, C.; Richter, S. *J. Am. Chem. Soc.* **2007**, *129*, 12352.
- (5) Giardi, M. T.; Pace, E. *Trends Biotechnol.* **2005**, *23*, 257.
- (6) Das, R.; Kiley, P. J.; Segal, M.; Norville, J.; Yu, A. A.; Wang, L.; Trammell, S. A.; Reddick, L. E.; Kumar, R.; Stellacci, F.; Lebedev, N.; Schnur, J.; Bruce, B. D.; Zhang, S.; Baldo, M. *Nano Lett.* **2004**, *4*, 1079.
- (7) Frolov, L.; Rosenwaks, Y.; Richter, S.; Carmeli, C.; Carmeli, I. *J. Phys. Chem. C* **2008**, *112*, 13426–30.
- (8) Avouris, P.; Freitag, M.; Perebeinos, V. *Nat. Photonics* **2008**, *2*, 341.
- (9) Dresselhaus, M. S.; Dresselhaus, G.; Eklund, P. C. *Science of Fullerenes and Carbon Nanotubes*; Academic: New York, 1996.
- (10) Zebli, B.; Vieyra, H. A.; Carmeli, I.; Hartschuh, A.; Kotthaus, J. P.; Holleitner, A. W. *Phys. Rev. B* **2009**, *79*, 205402.
- (11) Hazani, M.; Hennrich, F.; Kappes, M.; Naaman, R.; Peled, D.; Sidorov, V.; Shvartz, D. *Chem. Phys. Lett.* **2004**, *391*, 389.
- (12) Guldi, D. M.; Rahman, G. M. A.; Sgobba, V.; Ehli, C. *Chem. Soc. Rev.* **2006**, *35*, 471.
- (13) Whalley, A. C.; Steigerwald, M. L.; Guo, X.; Nuckolls, C. *J. Am. Chem. Soc.* **2007**, *129*, 12590–12591.
- (14) Carmeli, I.; Mangold, M.; Frolov, L.; Zebli, B.; Carmeli, C.; Richter, S.; Holleitner, A. W. *Adv. Mater.* **2007**, *19*, 3901.
- (15) Kaniber, S. M.; Simmel, F. C.; Holleitner, A. W.; Carmeli, I. *Nanotechnol.* **2009**, *20*, 345701.
- (16) Freitag, M.; Martin, Y.; Misewich, J. A.; Martel, R.; Avouris, Ph. *Nano Lett.* **2003**, *3*, 1067.
- (17) Kataura, H.; Kumazawa, Y.; Maniwa, Y.; Umezumi, I.; Suzuki, S.; Ohtsuka, Y.; Achiba, Y. *Synth. Met.* **1999**, *103*, 2555–2558.
- (18) Kaniber, S. M.; Song, L.; Kotthaus, J. P.; Holleitner, A. W. *Appl. Phys. Lett.* **2009**, *94*, 261106.
- (19) Hernández-Martínez, P. L.; Govorov, A. O. *Phys. Rev. B* **2008**, *78*, 035314.

JA910790X